Eigencurrent Analysis of Resonant Behavior in Finite Antenna Arrays

Dave J. Bekers, *Member, IEEE*, Stephanus J. L. van Eijndhoven, Alphons A. F. van de Ven, Peter-Paul Borsboom, and Anton G. Tijhuis, *Member, IEEE*

***Abstract*—Resonant behavior in a finite array that appears as (modulated) impedance or current-amplitude oscillations may limit the array bandwidth substantially. Therefore, simulations should predict such behavior. Recently, a new approach has been developed, called the eigencurrent approach, which can predict resonant behavior in finite arrays. A study of line arrays of either E- or H-plane-oriented strips and rings in free space and in half-spaces confirms our conclusion in earlier research that resonant behavior is caused by the excitation of one of the eigencurrents. The eigenvalue (or characteristic impedance) of this eigencurrent becomes small in comparison to the eigenvalues of the other eigencurrents that can exist on the array geometry. We demonstrate that the excitation of this eigencurrent results in an edge-diffracted wave propagating along the surface of the array, which may turn into a standing wave. In that case, the amplitudes and phases of the element impedances show the same standing-wave pattern as those of the excited eigencurrent. We demonstrate that the phase velocity of this wave is approximately equal to or slightly larger than the free-space velocity of light. Finally, we throw light on the relation between the excitation of eigencurrents with a small eigenvalue and the behavior of super directive arrays.**

***Index Terms*—Antenna arrays, eigencurrent, resonance, standing wave.**

I. Introduction

DESIGNS of antenna arrays are often based on simulations of infinite periodic arrays, where symmetry is used to restrict the analysis to a single element. Such simulations are much less computationally expensive than the brute-force numerical approaches applied to a complete array. Since all element currents are the same, the simulations do not reveal resonant array behavior that appears as impedance or current-amplitude oscillations along the elements of a finite array [1]–[3]. Such behavior may reduce the performance of an array considerably and therewith its bandwidth [4]. Consequently, an accurate prediction of resonant behavior is necessary.

Numerous approaches were developed to efficiently compute the electromagnetic behavior of finite arrays [5]–[9][10]. These approaches, however, do not provide a means to trace resonant behavior. Moreover, most of the approaches are based on assumptions that exclude (large) variations of element impedances and currents along the array. For example, in [6], the assumption of slow variation of the element impedances is used and in [5, Sec. VIII], the currents on elements that are typically at least three or four elements away from the edges of the array are computed by the infinite-array approach.

Only a few approaches were developed to trace resonant behavior. In [3], resonant behavior due to traveling waves along the surface of an array is studied by decomposing the element currents into Floquet currents (on the corresponding infinite array), currents associated with surface waves, and residual currents. Note that surface-wave behavior has been found experimentally in [11]. The resonant behavior in [3] occurs at frequencies 10%–20% below the frequency for which the array exhibits a "resonant broadside embedded impedance," i.e., the frequency f_{RBEI} for which the element reactances are, on average, zero. In this sense, the behavior differs from the resonant behavior described in [1] and [2], which occurs near f_{RBEI}.

Recently, source-free solutions of Maxwell's equations that represent traveling waves on infinite arrays have been explored to find an explanation for resonances that occur in finite axial arrays of closely spaced loop antennas [12]. These solutions, or modes, are determined from a homogeneous matrix equation that results from collocation applied to eigenfunction expansions of the electromagnetic field. It is suggested that the lowest order mode on the infinite array is the dominant mechanism of a finite array resonance observed in a specific finite axial array of loop antennas. In this respect, we note that the traveling wave represented by this mode turns into a standing wave on the finite array and, thus, causes the mentioned impedance and current-amplitude oscillations.

In [13] and [14], we proposed an approach to simulate the behavior of finite arrays. The approach, which we called the eigencurrent approach, leads to rapidly executable simulations and can predict resonant behavior in finite arrays [4], [14, Ch. 6]. In this paper, we first present an outline of the eigencurrent approach. Subsequently, we study resonant behavior in planar uniform line arrays of ring-shaped microstrips (shortly rings) and of parallel rectangular microstrips (shortly strips) in two different ways. The first way is by application of the eigencurrent analysis [4], [14, Ch. 6]. The second way is by an investigation of the phases of the current distributions on line arrays of which only one of the outer elements is excited. Finally, we comment on parameter dependence and sensitivity of the resonant behavior.

Manuscript received October 3, 2005; revised February 24, 2006. This work was supported by Thales Nederland and by the Stan Ackermans Institute, Technische Universiteit Eindhoven.

D. J. Bekers is with TNO Defence, Security, and Safety, 2509 JG Den Haag, The Netherlands (e-mail: dave.bekers@tno.nl).

S. J. L. van Eijndhoven and A. A. F. van de Ven are with the Faculty of Mathematics and Computer Science, Technische Universiteit Eindhoven, 5600 MB Eindhoven, The Netherlands.

P.-P. Borsboom is with SARA Computing and Networking Services, 1090 GP Amsterdam, The Netherlands.

A. G. Tijhuis is with the Faculty of Electrical Engineering, Technische Universiteit Eindhoven, 5600 MB Eindhoven, The Netherlands.

Digital Object Identifier 10.1109/TMTT.2006.875446

0018-9480/$20.00 © 2006 IEEE

II. Eigencurrent Approach

In the eigencurrent approach, the behavior of a finite array is described by its eigenvibrations or eigencurrents. These eigencurrents are the eigenfunctions of the impedance operator that relates the current on the array to its excitation field. From a physical point-of-view, the eigencurrents are standing waves of the array. The corresponding eigenvalues represent the characteristic impedances of the eigencurrents. The larger the characteristic impedance of an eigencurrent, the less this eigencurrent contributes to the current. The concept of eigencurrent turns out to be extremely suitable for the design of arrays because the design characteristics and the excitation of specific eigencurrents are one-to-one related. Analysis of the spectrum of the impedance operator, as described in [14], reveals that eigencurrents and corresponding eigenvalues are one-to-one related to sum patterns, to difference patterns, to grating lobes, to modulated impedance oscillations, to impedance variations attributed to surface waves, and to many other properties of the array.

The first step of the approach is the determination of the spectrum of a single element. Element eigenvalues and element eigencurrents are computed from a "normalized" moment matrix related to chosen expansion functions for the current on the element. For a ring element, the element eigencurrents are known analytically: $1, \cos n\varphi, \sin n\varphi (n = 1, 2, \ldots)$, where φ is the circumferential angle. Subsequently, an inner product is determined for which the element eigencurrents are orthonormal, yielding a diagonal moment matrix.

In the second step, the spectrum of the array is determined. On each element, the array eigencurrents are described by linear expansions of the element eigencurrents. The expansion coefficients of the array eigencurrents and their eigenvalues are the eigenvectors and eigenvalues of a moment matrix for the array. In the computation of this matrix, the expansion and test functions are the element eigencurrents, and the inner product is the composition of the element inner products determined in the first step. The array eigencurrents and their eigenvalues are divided into groups, where each group corresponds to a single element eigencurrent. This eigencurrent describes the dominant behavior of the array eigencurrents in the group. The corresponding array eigenvalues evolve from the eigenvalue of the dominant element eigencurrent.

The numerical effort in the eigencurrent approach is significantly reduced by computing the moment matrix for the array with only those element eigencurrents that contribute to mutual coupling. The groups of array eigencurrents and array eigenvalues corresponding to these element eigencurrents are thus computed from a reduced moment matrix. The groups of array eigenvalues and array eigencurrents corresponding to the other element eigencurrents follow without numerical computation. For details, we refer to [14, Ch. 5].

By the eigencurrent approach, the current $\boldsymbol{J}$ on the elements of a finite array is found as

$$\boldsymbol{J} = \sum_{n=1}^{N} \sum_{q=1}^{Q} \frac{1}{\nu_{nq}} \langle \boldsymbol{u}_{nq}, \boldsymbol{E}^{\mathrm{ex}} \rangle \, \boldsymbol{u}_{nq}. \tag{1}$$

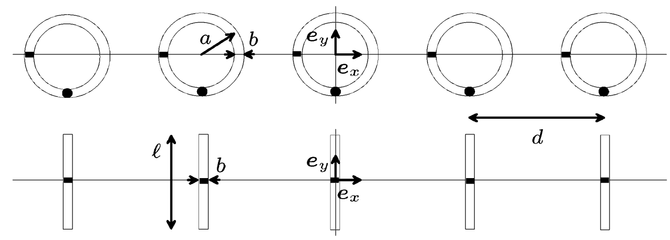

Fig. 1. Line array of rings and a line array of strips. The rings and strips are excited by voltage gaps. For the (H-plane-oriented) strips, the positions of these gaps are indicated by black rectangles. For H-plane-oriented rings, the positions are similarly indicated, while for E-plane-oriented rings, they are indicated by black circles.

Here, $\{\nu_{nq}\}_{q=1}^{Q}$ and $\{\boldsymbol{u}_{nq}\}_{q=1}^{Q} (n = 1, \ldots, N)$ are the groups of array eigenvalues and array eigencurrents, $\boldsymbol{E}^{\mathrm{ex}}$ is the tangential excitation field, Q is the number of elements, and the inner product $\langle \cdot, \cdot \rangle$ orthonormalizes the array eigencurrents. Moreover, N is the number of element eigencurrents, which depends on the number of expansion functions used. From (1), it is clear that a group of eigenvalues $\{\nu_{nq}\}_{q=1}^{Q}$ corresponding to a larger element eigenvalue, in general, contributes less to the current than a group corresponding to a smaller one. The ring and strip elements considered in this paper are typically designed to excite a single element eigencurrent. Consequently, the element currents are predominantly described by the first group of eigenvalues ($n = 1$), where we index the groups according to increasing element eigenvalues. We note that the rings and strips are chosen as array elements because the element eigencurrents of a single ring are known analytically and the strip is one of the simplest element geometries for which the element eigencurrents must be determined by computational methods.

III. Resonant Behavior in Arrays

Fig. 1 shows the geometry of the line arrays of rings and of strips. The line arrays are either in free space or in a homogeneous half-space at a distance h above an infinitely wide perfectly conducting ground plane. The surfaces of the elements are parallel to the plane and they are modeled as perfectly conducting and infinitely thin. Moreover, the width b of the elements is much smaller than the wavelength, while the spacing d, ring radius a, and strip length ℓ are of the same order of magnitude as the wavelength. The elements are excited by voltage gaps with equal phase and amplitude, as indicated in Fig. 1. As in [14], the currents on the rings are averaged with respect to their widths. Consequently, these currents are described by integro-differential equations with logarithmically singular kernels.

In [14, Fig. 2], we demonstrated resonant behavior in a line array of 40 H-plane-oriented rings in free space and in two half-spaces. In free space, this behavior occurs for the frequencies with $ka = 0.971$ and $ka = 0.943$, where k is the wavenumber. Since f_{RBEI} corresponds to $ka = 1.111$, the resonant behavior occurs 12.6% and 15.2% below this frequency. For the two half-spaces, these percentages reduce to approximately 2.8%. Here, we first consider the same array, but the rings are E-plane oriented and the array is positioned in a half-space with $h/a = 1.5$.

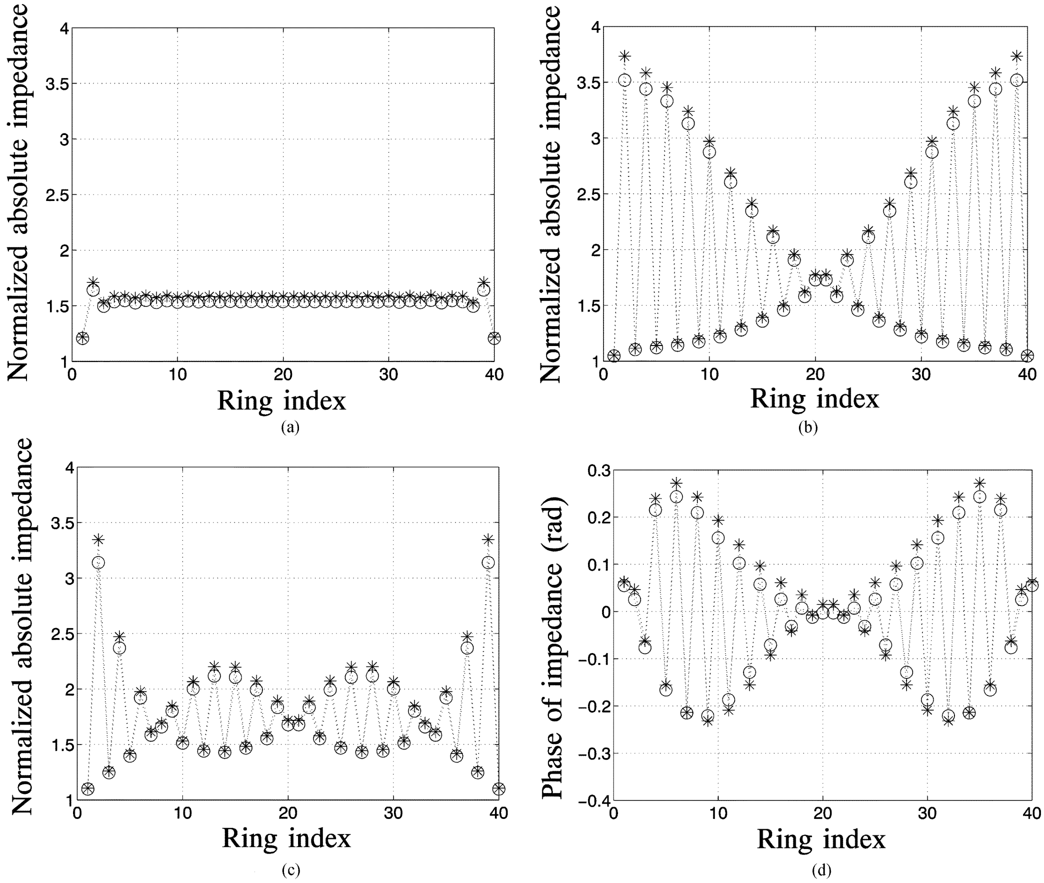

Fig. 2. Normalized ring impedances for a line array of 40 E-plane-oriented rings in a half-space excited by voltage gaps of 1 V at the frequencies with: (a) $ka = 1.0786$, (b) $ka = 1.0441$, and (c) $ka = 1.0378$. (d) Phases for $ka = 1.0378$. Impedances computed by the moment method ($*$) and by the eigencurrent approach ($\circ$). Normalization: for each frequency, the corresponding absolute impedance of a single ring. Parameter values: $d/a = 3$ ($d = \lambda/2$ at $ka = 1.047$), $b/a = 0.06, h/a = 1.5$.

In Fig. 2, we depict the normalized absolute impedances for the frequencies with $ka = 1.0786, ka = 1.0441$, and $ka = 1.0378$, computed by the moment method and by the eigencurrent approach. For $ka = 1.0786$, the (absolute) impedance pattern is almost uniform, while for the other two frequencies, the pattern exhibits large modulated oscillations of the same shape as in [4, Fig. 2] for H-plane-oriented rings in free space. The phase pattern in Fig. 2(d) reveals that the phase distribution along the array is, on average, approximately zero at $ka = 1.0378$. The same is valid for $ka = 1.0441$, which indicates that $f_{\rm RBEI}$ corresponds to approximately $ka = 1.04$. Hence, while the resonant behavior for the H-plane-oriented rings in free space and in two half-spaces occurs below $f_{\rm RBEI}$, the resonant behavior for the E-plane-oriented rings in a half-space occurs at $f_{\rm RBEI}$.

The moment-method result in Fig. 2 is generated with eight cosine/sine expansion functions prescribed on each ring. These functions are the element eigencurrents, and are used as such in the eigencurrent approach. Hence, $N = 8$ in (1). The reduced moment matrix is computed with only two element eigencurrents. The other six element eigencurrents are assumed not to contribute to the mutual coupling. The match between the results of the moment method and the eigencurrent approach illustrate the validity of this assumption. For a verification of our moment-method code by comparison with results in the literature, we refer to [14, Sec. 2.5].

Similar modulated oscillations are observed in a line array of 40 parallel, or H-plane-oriented, strips in free space for $\ell/\lambda = 0.429$ and $\ell/\lambda = 0.425$ (modulation with a sine of 1 and 2 periods, respectively). Note that $\ell/d = 0.992$ and $b/\ell = 0.02$. Since $f_{\rm RBEI}$ corresponds to $\ell/\lambda = 0.496$, the resonant behavior occurs 13.6% and 14.4% below this frequency. These percentages are comparable to those mentioned at the beginning of this section for the line array of 40 H-plane-oriented rings in free space in [4]. For the same array of strips, but positioned in a half-space with $h/\ell = 0.4$, $f_{\rm RBEI}$ corresponds to $\ell/\lambda = 0.468$, while the modulated oscillations appear at $\ell/\lambda = 0.441$ and $\ell/\lambda = 0.439$, i.e., 5.6%, and 6.2% below $f_{\rm RBEI}$. Moreover, tests for the same array as in Fig. 2, but positioned in free space reveal that resonant behavior occurs at $f_{\rm RBEI}$, but this behavior is not nearly as pronounced as in a half-space. These results suggest that for H-plane-oriented elements, the ground plane shifts the frequencies at which the resonant behavior occurs towards $f_{\rm RBEI}$, while for E-plane-oriented elements, the ground plane is essential for the occurrence of this behavior.

Finally, we note that in [1] and [2], resonant behavior is observed at $f_{\rm RBEI}$ for line arrays of E-plane-oriented, or collinear, strips in a half-space. The behavior is explained by a traveling wave between the array and ground plane. Our results show that the presence of a ground plane is not essential for the occurrence of the behavior.

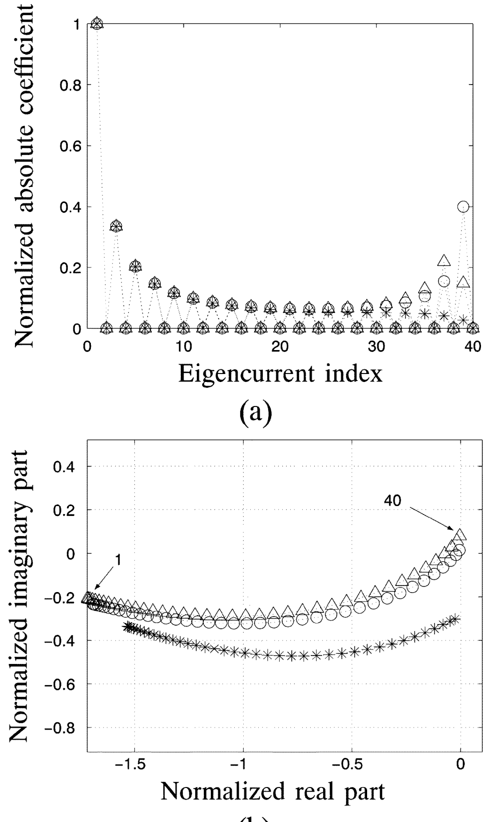

Fig. 3. (a) Normalized absolute coefficients in the finite expansion (1) of the current and (b) normalized eigenvalues of the first group for the line array in Fig. 2 for the frequencies with $ka = 1.0378(\triangle), ka = 1.0441(\circ), ka = 1.0786(*)$. The eigenvalues describe curves in the complex plane of which the 1st and 40th eigenvalue are indicated. Normalization: for each frequency, (a) the maximum absolute coefficient and (b) the corresponding absolute element eigenvalue.

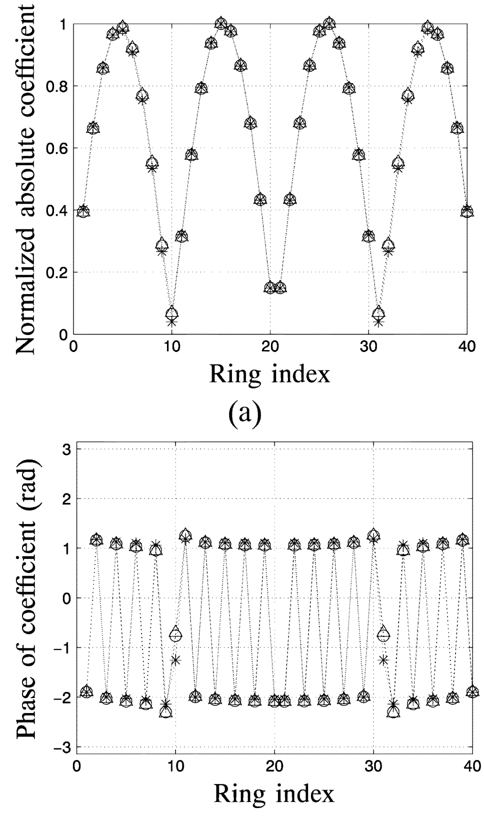

Fig. 4. (a) Normalized absolute values and (b) phases of the coefficients of the dominant element eigencurrents in the 37th eigencurrent of the first group for the line array in Fig. 2 for the frequencies with $ka = 1.0378(\triangle), ka = 1.0441(\circ), ka = 1.0786(*)$. Normalization: maximum absolute coefficient.

IV. Explanation of Resonant Behavior by Eigencurrent Analysis

As demonstrated in [4], the resonant behavior occurs because the eigenvalue of one of the array eigencurrents, called the resonant eigencurrent, becomes small with respect to the eigenvalues of the other array eigencurrents. Therefore, the contribution of the corresponding array eigencurrent in (1) is larger than that of other eigencurrents, although its phase distribution does not "fit" at all to the uniform phase distribution of the excitation. Figs. 3 and 4 illustrate these conclusions for the line array in Fig. 3. Fig. 3 shows the normalized absolute expansion coefficients in (1) for the first group of array eigencurrents, i.e., $\{\langle \boldsymbol{u}_{1q}, \boldsymbol{E}^{\mathrm{ex}}\rangle / \nu_{1q}\}_{q=1}^{40}$. Note that the behavior of the coefficients is similar to the behavior, at different frequencies, of those for the line array of H-plane-oriented rings shown in [4, Fig. 3]. For $ka = 1.0786$, the coefficients with even indices are zero, while those with odd indices form a monotonically decreasing sequence. The coefficients with even indices are zero because the corresponding array eigencurrents are antisymmetric along the array. Moreover, the first array eigencurrent is excited most because its coefficients of the dominant element eigencurrents exhibit a uniform phase pattern, which "fits" to the uniform phase pattern of the excitation [14]. For $ka = 1.0441$ and $ka = 1.0378$, the coefficients show the same behavior as the coefficients for $ka = 1.0786$, but for $ka = 1.0441$, the 39th array eigencurrent has a larger coefficient, while for $ka = 1.0378$, both the 37th and 39th array eigencurrent have a larger coefficient. Fig. 3(b) confirms that the corresponding eigenvalues become small with respect to the other eigenvalues. For the same array, but positioned in free space, the eigenvalues follow approximately the same curves as in Fig. 3(b), but none of the eigenvalues becomes really small with respect to the other eigenvalues. Therefore, the resonant behavior is not nearly as pronounced as in a half-space.

Fig. 4 shows the distribution of the coefficients of the dominant element eigencurrents in the 37th array eigencurrent. For the E-plane-oriented rings, the dominant element eigencurrent is $\sin\varphi$ with φ being the angle with respect to the axis of the line array and $\varphi = 3\pi/2$ being the position of the voltage gaps. Recall that for the H-plane-oriented rings in [4], the dominant element eigencurrent is $\cos\varphi$ with $\varphi = \pm\pi$ being the position of the voltage gaps. Fig. 4 confirms the statement in [14] and [4] that the array eigencurrents depend negligibly on the frequency; not only the coefficients, but also the dominant element eigencurrents are the same for the three frequencies under consideration. Since the array eigencurrents also depend negligibly on the element shape, the 39th array eigencurrent for this case is the same as the 39th array eigencurrent in [4, Fig. 4] for the line array of H-plane-oriented rings. Fig. 4 and [4, Fig. 4] confirm that the phase distributions of the 37th and 39th array eigencurrent do not "fit" to the uniform phase distribution of the excitation. Moreover, the absolute sine-like amplitude patterns of one and two periods of the 39th and 37th array eigencurrent, respectively, can be clearly observed in the impedance patterns of Fig. 2(b) and (c).

V. Explanation of Resonant Behavior in Terms of Surface-Wave Excitation

In [2], the modulations of the impedance are explained by an edge diffracted wave propagating along the array somewhat faster than the free-space phase velocity. To estimate this phase velocity for line arrays of wires, only one of the outer wires is excited. The resulting currents in the middle of the wires are written as

$$I_n = A_n \exp(-j(n-1)kd(1-\epsilon)), \tag{2}$$

where ϵ is small, A_n is the amplitude of the current, and n is the wire index. Next, the phases of these currents are divided by the free-space phase factor $\exp(-j(n-1)kd)$ to estimate the factor ϵ.

Following [2] for the line array of E-plane-oriented rings in a half-space in Section III, we excite only the first ring by a voltage gap of 1 V. In the original positions of the excitations, we then obtain similar amplitude and phase distributions for the current as in [2]. For the modulations at $ka = 1.0378$, these distributions are shown in Fig. 5. The current amplitudes decrease almost monotonically, while the phases, after division by $\exp(-j(n-1)kd)$, increase linearly. Since the slope of the curve in Fig. 5 is approximately 0.212 rad, we obtain $\epsilon \approx 0.0621$. According to [2], the period of the modulation of the impedance is estimated by $2/\epsilon \approx 29.6$, which is a reasonable approximation of the period estimated from Fig. 2(c), i.e., 27.

Next, we consider the same line array, but with H-plane-oriented rings (as in [4]), $h/a = 1.2$ instead of $h/a = 1.5$, and $ka = 0.990$. The array shows a similar modulated (absolute) impedance pattern as in Fig. 2(b) and (c); (see [4, Fig. 6]). The results of Fig. 6 show that the amplitudes of the current have the same behavior as in Fig. 5, but the phases do not increase linearly at all. A closer look at the different array geometries reveals that, for the array with E-plane-oriented rings and for the line arrays of collinear strips in [2], the spacing between the elements equals $\lambda/2$ or $kd = \pi$. Hence, the current is divided by $\exp(-j(n-1)\pi)$. Dividing the current on the array with H-plane-oriented rings by $\exp(-j(n-1)\pi)$ as well, we obtain the same linear phase pattern as obtained for E-plane-oriented rings, see Fig. 7(a). This is not surprising since, for both arrays, the 37th array eigencurrent is excited and the coefficient distribution of the dominant element eigencurrent is the same for both arrays. Dividing the coefficients of the 37th array eigencurrent by $\exp(-j(n-1)\pi)$, we obtain the phase pattern in Fig. 7(b). Combining this phase pattern with the amplitude pattern in Fig. 4(a), we observe that the eigencurrent coefficients follow a standing-wave pattern, i.e., a sine of two periods. The total phase shift of this pattern equals 3π, which is larger than

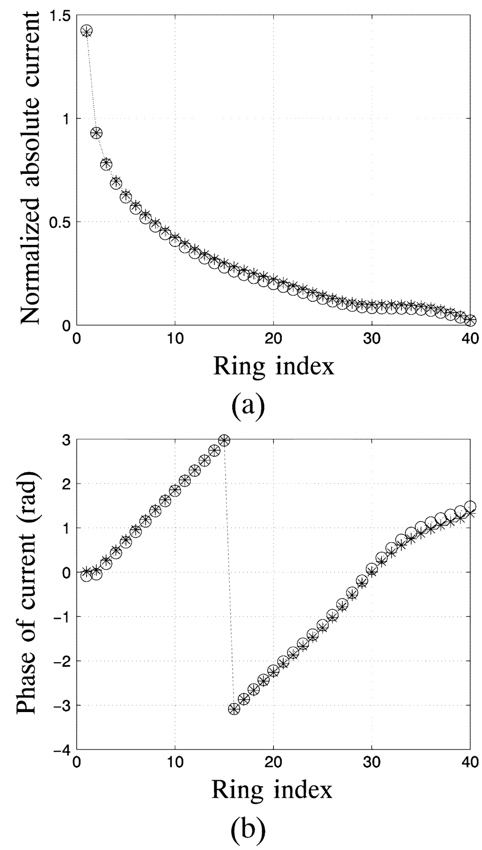

Fig. 5. (a) Current amplitudes and (b) corresponding phases (after division by $\exp(-j(n-1)kd)$) in the excitation positions of the line array in Fig. 2. Only the first ring is excited by a voltage gap of 1 V at the frequency with $ka = 1.0378$. Currents computed by the moment method ($*$) and by the eigencurrent approach ($\circ$). Normalization: the corresponding current amplitude of a single ring.

the total phase shift of approximately 2.5π of the linear phase progression in Figs. 5(b) and 7(a). The reason is that in case only the first ring of the array is excited, the 38th eigencurrent is as much as excited as the 37th eigencurrent. The coefficients of the dominant element eigencurrents in the 38th array eigencurrent, divided by $\exp(-j(n-1)\pi)$, constitute a sine pattern of 1.5 periods with a total phase shift of 2π. Consequently, the linear phase progression of the current "fits" to the block-like phase distributions of both the 37th and 38th eigencurrent.

The linear phase progressions shown in Figs. 5(b) and 7(a) suggest that a wave is propagating along the array surface with phase increment $\pi(1-\epsilon)$. Its phase velocity equals $2dc_0/(1-\epsilon)\lambda$, where c_0 is the free-space velocity of light. For a half-wavelength spacing, this phase velocity equals the phase velocity predicted in [2], i.e., $c_0/(1-\epsilon)$. Hence, for the line array of E-plane-oriented rings, the phase velocity is slightly larger than c_0: $1.066\,c_0$. For the line array of H-plane-oriented rings, the phase velocity is $1.007\,c_0$ since $2d/\lambda = 0.945$ and $1-\epsilon = 0.941$. In the same way, we computed the phase velocities of the waves along the arrays in free space. For example, for the line array of H-plane-oriented rings in free space in [4, Fig. 2], the phase velocity corresponding to the impedance pattern modulated by the 37th eigencurrent is $0.993\,c_0$ since $2d/\lambda = 0.900$ and $\epsilon \approx 0.094$.

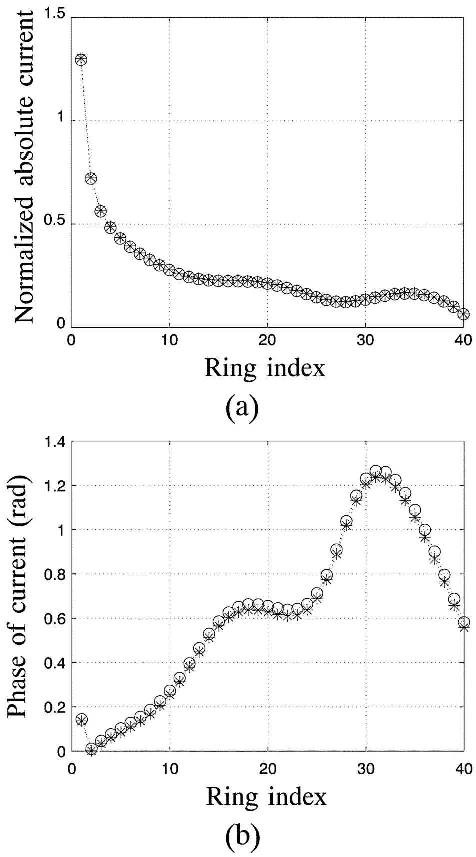

Fig. 6. As Fig. 5, but the rings are H-plane oriented, $h/a = 1.2$, and the frequency is such that $ka = 0.990$.

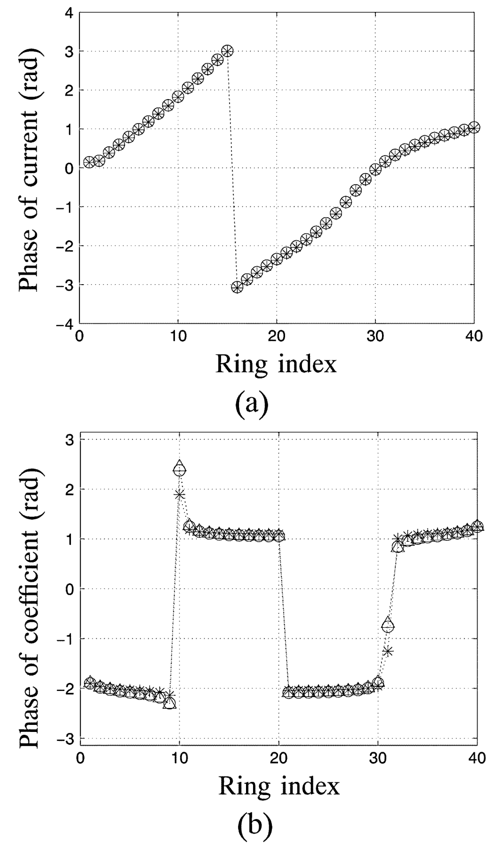

Fig. 7. (a) As Fig. 6(b), but the currents are divided by $\exp(-j(n-1)\pi)$ instead of $\exp(-j(n-1)kd)$. (b) As Fig. 4(b), but the coefficients are divided by $\exp(-j(n-1)\pi)$.

We also investigated impedance patterns modulated by the 39th eigencurrent as, for example, shown in Fig. 2(b) for E-plane-oriented rings. Here, we show results for the array of H-plane-oriented rings in Figs. 6 and 7 for $ka = 0.995$. Fig. 8 shows the amplitudes and phases of the currents in the original excitation positions, where only the first ring is excited by a voltage gap. Instead of a monotonically decreasing amplitude, we observe clearly an absolute sine-like pattern. Moreover, the phase does not increase linearly, but shows a kind of step pattern. Hence, in this case, the edge-diffracted wave propagating along the array turns into a standing wave. We observed that the 39th eigenvalue is close to zero in comparison to the other eigenvalues. Moreover, the amplitudes and phases of the current approximate the amplitudes and phases of the eigencurrent coefficients of the dominant element eigencurrent in the 39th array eigencurrent. Those coefficients, divided by $\exp(-j(n-1)\pi)$, show a sine pattern of one period. For the frequency range in which the impedances are modulated by the 37th eigencurrent, we did not find a frequency at which the propagating wave turns into a standing wave. Apparently, the 37th eigenvalue does not become small enough. Increasing the line-array size from 40 to 100 rings, we did find such a frequency, as illustrated by Fig. 9(a) and (b). Fig. 9(a) shows the modulated (absolute) impedance for the uniformly excited array at $ka = 0.995$. If only the first ring is excited by a voltage gap, we obtain the standing-wave pattern in Fig. 9(b) for the current in the original excitation positions of the line array. The relative differences in Fig. 9(a) between the normalized peak impedances computed by the eigencurrent approach and those computed by the moment method are larger than the corresponding relative differences in Fig. 2. The eigenvalue corresponding to the resonant behavior in the first figure is closer to zero than the one corresponding to the second figure and, hence, the numerical approximation of the current is more sensitive to computational errors. However, this observation does not completely explain the larger relative differences since, in Fig. 9(a), the normalized impedances computed by the eigencurrent approach and those computed by the moment method match perfectly for magnitudes smaller than three. To compute the impedances of the elements, we invert the current values in the positions of the voltage gaps. The current values corresponding to the normalized peak impedances in Fig. 9(a) are closer to zero than those in Fig. 2 and, hence, may have larger relative approximation errors. Consequently, the relative differences between the normalized peak impedances computed by the eigencurrent approach and those computed by the moment method may be larger.

The remaining question is why a certain eigencurrent becomes resonant for a certain array geometry and frequency or why an edge-diffracted wave is launched along an array. For line arrays of H-plane-oriented strips or rings in free space or in a half-space, we found different frequencies at which resonant behavior occurs. This suggests that the occurrence of resonant behavior depends on the element shape and the spacing in

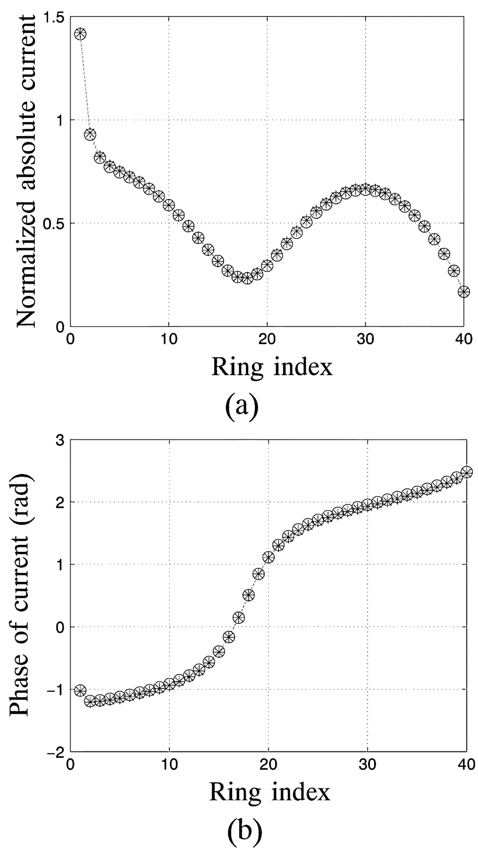

Fig. 8. As Fig. 5, but the frequency is such that $ka = 0.995$ and the phases of the current are divided by $\exp(-j(n-1)\pi)$ instead of $\exp(-j(n-1)kd)$.

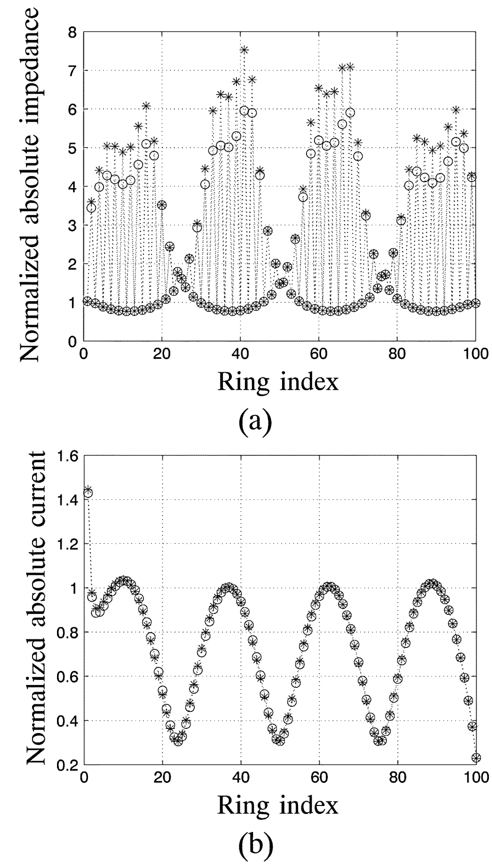

Fig. 9. Normalized absolute ring impedances for a line array of 100 H-plane-oriented rings in a half-space. The frequency is such that $ka = 0.995$. (a) All rings excited by voltage gaps of 1 V. (b) Only the outer left ring is excited. Currents computed by the moment method $(*)$ and by the eigencurrent approach $(\circ)$. Parameter values: $d/a = 3, b/a = 0.06, h/a = 1.2$.

the array and, consequently, on the near-field characteristics of the element in the array. We also observed that the frequencies at which standing-wave behavior occurs vary slightly with the array size, but the frequency range in which resonant behavior occurs does not. This suggests that the occurrence of resonant behavior depends little on the array length.

The resonant behavior studied here corresponds to the behavior of super directive arrays, as studied theoretically in [15] and [16] and experimentally in [17]. As stated in [15], such arrays are characterized by the elements, or sections of elements, being excited out of phase, where the spacing is less than $\lambda/2$. The eigencurrents that cause the resonant behavior we describe exactly show such a phase distribution [see, e.g., the distribution in Fig. 4(b)]. The magnitudes of the corresponding eigenvalues, located near the origin of the complex plane, vary rapidly as a function of the frequency [see Fig. 3(b)]. This result suggests a rapid increase and decrease of the magnitude of the current and, therewith, a high-Q resonance, as in super-directive arrays. In [16], amplitude and phase distributions are shown for high directive circular arrays, which are driven by a single element only. These distributions show the same patterns as the distributions shown in Figs. 8 and 9(b). Moreover, comparing the distributions in [16] with the amplitude and phase distributions of eigencurrents, as described in detail in [14, Ch. 5], we observe that the elements in the array are grouped in the same way. These comparisons demonstrate that high and super-directive behavior is obtained by the excitation of a single eigencurrent with a small eigenvalue. Finally, as observed in [4], the behavior of the eigenvalues in the complex plane can be used to predict resonant behavior. Since the deformation and translation of the eigenvalue curve in the complex plane is gradual, only two or three simulations may indicate for which frequency resonant behavior can be expected. This feature of the eigencurrent approach may facilitate not only the prediction of resonant behavior, but also the design of super directive arrays. Further research in this direction is necessary.

VI. Parameter Dependence and Sensitivity

In [1] and [2], it is demonstrated that the period of modulation of the element impedances depends on the wire radius. We found such a dependence as well, but not for all array geometries and frequencies. The presence and absence of such a dependence is due to the presence of a relatively small eigenvalue, by which the current distribution is sensitive to small parameter variations. This observation raises the question what happens to the modulated impedance behavior when the array geometry is randomly perturbed, as in practice. We consider the line array in Fig. 2 excited at $ka = 1.0378$. The impedances of the rings then show the modulated pattern in the lower two pictures of Fig. 2. As an example, we consider the following parameter choice for a design at 1 GHz: $a = 50$ mm, $b = 3$ mm, $d = 150$ mm, and $h = 75$ mm. Let us assume that the microstrip structures are

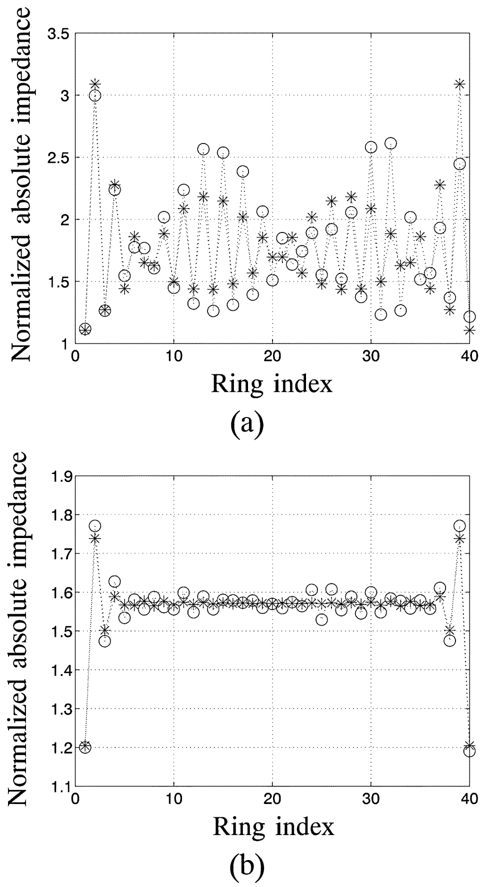

Fig. 10. Normalized absolute ring impedances for a line array of 40 E-plane-oriented rings in a half-space excited by voltage gaps of 1 V at: (a) $ka = 1.0378$ and (b) $ka = 1.0786$. The array geometry is either uniform $(*)$ or perturbed $(\circ)$ with a small random perturbation on radii, widths, and centers. Normalization: for each frequency, the corresponding absolute impedance of a single ring. Parameter values: $d/a = 3, b/a = 0.06, h/a = 1.5$.

produced with an accuracy of 0.1 mm. The radius a, width b, and positions of the centers of the rings then exhibit a random error of, at most, 0.1 mm. We assume that the heights of the rings above the ground plane are not perturbed. Fig. 10(a) shows the normalized absolute impedances of the rings for both the uniform array and randomly perturbed array. We observe that the resonant behavior persists and, hence, that the eigenvalue of the resonant eigencurrent is not so much affected that it is no longer small with respect to the other eigenvalues. For comparison, Fig. 10(b) shows the normalized absolute impedances for the same array, but at $ka = 1.0786$. The absolute impedances of the uniform line array are only slightly perturbed.

VII. Conclusion

In this paper, we have demonstrated that resonant behavior in finite arrays is caused by the excitation of one of the eigencurrents of the array. The characteristic impedance, or eigenvalue, of this eigencurrent becomes small in comparison to the characteristic impedances of the other eigencurrents that can exist on the array geometry. We have demonstrated that the excitation of this eigencurrent results in an edge-diffracted wave along the surface of the array. This wave may turn into a standing wave. In that case, the amplitudes and phases of the element impedances show the same standing-wave pattern as those of the excited eigencurrent. We have demonstrated that the phase velocity of the wave is approximately equal to or slightly larger than the free-space velocity of light. Such a demonstration is described in the literature, but our demonstration is valid for a wider range of arrays. Finally, we have demonstrated that the resonant behavior we observe corresponds to the behavior of super-directive arrays demonstrates, which exhibit resonant behavior of high Q. In particular, super-directive behavior is obtained by exciting a single eigencurrent with a relatively small characteristic impedance.

We have arrived at the conclusions stated above by investigating resonant behavior in planar line arrays of rings and strips in free space and half-spaces, which appears as modulated oscillations of the element impedances. In free space, the frequency at which this behavior occurs is 10%–20% below the frequency f_{RBEI} for which the array exhibits a "resonant broadside embedded impedance," while in a half-space, this behavior occurs just below or at f_{RBEI}. Moreover, for E-plane-oriented elements, the presence of a ground plane seems to be essential for the occurrence of resonant behavior, while for H-plane-oriented elements, the behavior occurs in free space as well as in half-spaces.

Acknowledgment

A portion of this research was carried out while author D. J. Bekers was with the Technische Universiteit Eindhoven, Eindhoven, The Netherlands.

References

[1] R. C. Hansen, "anomalous edge effects in finite arrays," *IEEE Trans. Antennas Propag.*, vol. 47, no. 3, pp. 549–554, Feb. 1999.

[2] C. Craeye and M. Arts, "Modulated oscillations appearing in the scan impedance of a finite phased array," *IEEE Trans. Antennas Propag.*, vol. 51, no. 9, pp. 2504–2506, Sep. 2003.

[3] B. A. Munk, *Finite Antenna Arrays and FSS*. New York: Wiley, 2003.

[4] D. J. Bekers, S. J. L. van Eijndhoven, A. A. F. van de Ven, P.-P. Borsboom, and A. G. Tijhuis, "Analysis of resonant behavior in planar line arrays of rings by the eigencurrent approach," in *Proc. 35th Eur. Microw. Conf.*, Paris, France, Oct. 2005, pp. 333–336.

[5] R. Mittra, C. H. Chan, and T. Cwik, "Techniques for analyzing frequency selective surfaces—A review," *Proc. IEEE*, vol. 76, no. 12, pp. 1593–1614, Dec. 1988.

[6] A. K. Skrivervik and J. R. Mosig, "Analysis of finite phase arrays of microstrip patches," *IEEE Trans. Antennas Propag.*, vol. 41, no. 8, pp. 1105–1114, Aug. 1993.

[7] G. A. E. Vandenbosch and F. J. Demuynk, "The expansion wave concept—Part II: A new way to model mutual coupling in microstrip arrays," *IEEE Trans. Antennas Propag.*, vol. 46, no. 3, pp. 407–413, Mar. 1998.

[8] A. Neto, S. Maci, G. Vecchi, and M. Sabbadini, "A truncated Floquet wave diffraction method for the full wave analysis of large phased arrays—Part I: Basic principles and 2D cases," *IEEE Trans. Antennas Propag.*, vol. 48, no. 3, pp. 594–600, Mar. 2000.

[9] O. AydinÇivi, P. H. Pathak, H.-T. Chou, and P. Nepa, "A hybrid uniform geometrical theory of diffraction—Moment method for efficient analysis of electromagnetic radiation/scattering from large finite planar arrays," *Radio Sci.*, vol. 35, no. 2, pp. 607–620, Mar.–Apr. 2000.

[10] C. Craeye, A. G. Tijhuis, and D. H. Schaubert, "An efficient MoM formulation for finite-by-infinite arrays of two-dimensional antennas arranged in a three-dimensional structure," *IEEE Trans. Antennas Propag.*, vol. 52, no. 1, pp. 271–281, Jan. 2004.

[11] H. W. Ehrenspeck and H. Poehler, "A new method for obtaining maximum gain from Yagi antennas," *IRE Trans. Antennas Propag.*, vol. AP-7, no. 4, pp. 379–386, Oct. 1959.

[12] S. Li and R. W. Scharstein, "Periodic structure eigenmodes for simple linear arrays," in *Proc. IEEE AP-S Int. Symp./USNC/URSI Nat. Radio Sci. Meeting*, Washington, DC, July 2005, p. 170.

[13] D. J. Bekers, S. J. L. van Eijndhoven, A. A. F. van de Ven, P.-P. Borsboom, and A. G. Tijhuis, "Modeling and analysis of finite phased arrays of microstrip antennas—An eigenvector approach," in *Proc. Int. Electromagn. Adv. Applicat. Conf.*, Turin, Italy, Sep. 2003, pp. 561–564.

[14] D. J. Bekers, *Finite Antenna Arrays: An Eigencurrent Approach*. Eindhoven, The Netherlands: Tech. Univ. Eindhoven. [Online]. Available: http://alexandria.tue.nl/extra2/200411410.pdf

[15] V. Veremey, "Superdirective antennas with passive reflectors," *IEEE Antennas Propag. Mag.*, vol. 37, no. 2, pp. 16–27, Apr. 1995.

[16] G. Fikioris, R. W. P. King, and T. T. Wu, "The resonant array of electrically short elements," *J. Appl. Phys.*, vol. 68, no. 2, pp. 431–439, July 1990.

[17] J. Shefer, "Periodic cylinder arrays as transmission lines," *IEEE Trans. Microw. Theory Tech.*, vol. MTT-11, no. 1, pp. 55–61, Jan. 1963.

Dave J. Bekers (M'06) was born in Breda, The Netherlands, in 1974. He received the M.Sc. degree in mathematics, P.Deng. degree, and Ph.D. degree from the Technische Universiteit Eindhoven, Eindhoven, The Netherlands, in 1999, 2001, and 2004, respectively.

He carried out his final project for the postgraduate program "Mathematics for Industry" and his Ph.D. project with Thales Nederland, Hengelo, The Netherlands, in the field of array antennas. Since November 2004, he has been with TNO Defence, Security, and Safety, Den Haag, The Netherlands.

Stephanus J. L. van Eijndhoven was born in Sint-Oedenrode, The Netherlands, in 1956. He received the M.Sc. degree in mathematics and Ph.D. degree from the Technische Universiteit Eindhoven, Eindhoven, The Netherlands, in 1979 and 1983, respectively.

Since 1983, he has been involved in the field of functional analysis. He is currently the Director of the postgraduate program "Mathematics for Industry" with the Technische Universiteit Eindhoven.

Alphons A. F. van de Ven received the M.Sc. degree in mechanical engineering and Ph.D. degree from the Technische Universiteit Eindhoven, Eindhoven, The Netherlands, in 1965 and 1975, respectively.

Since 1985, he has been an Associate Professor with the Centre for Analysis, Scientific Computing, and Applications (CASA) Group, Department of Mathematics and Computer Science, Technische Universiteit Eindhoven, where he has specialized in continuum mechanics and industrial mathematics. He teaches in theoretical mechanics and continuum mechanics, and he performs research in continuum mechanics, inclusive of interactions in thermal and electromagnetic fields. One of his current fields of interest is the flow behavior of polymer melts and blends. He is the coordinator of the T-stroom (orientation towards technical applications) of the postmaster programme "Mathematics for Industry." As such, he presents a course on mathematical physics/industrial mathematics entitled "Modeling and Mathematical Solution Techniques" and he supervises modeling projects and final projects. He is a member of the research school Engineering Mechanics (EM) and member of the Editorial Board of the *Journal of Engineering Mathematics*. He has supervised a series of masters projects, and has been involved, either as co-promotor or committee member in several doctoral projects.

Peter-Paul Borsboom was born in Rijswijk (Z-H), The Netherlands, in 1966. He received the M.Sc. degree in applied physics and Ph.D. degree from Delft University of Technology, Delft, The Netherlands, in 1989 and 1994, respectively. His thesis was entitled "Field Analysis of Integrated Optical Gratings."

From 1994 to 1997 , he was involved with the modeling of the scattering of radio waves by two-dimensional objects as a Higher Scientific Officer with the Rutherford Appleton Laboratory, Chilton, U.K. From 1997 to 2005, he participated in the research and development of phased-array systems with Thales Nederland BV, by modeling array antennas in their complex environments, and as member of the antenna and system engineering teams. In 2005, he became a consultant with SARA Computing and Networking Services, Amsterdam, The Netherlands. He is currently involved with a solution to manage and store massive data streams generated by the LOFAR radio telescope currently being developed in The Netherlands.

Anton G. Tijhuis (M'88) was born in Oosterhout N.B., The Netherlands, in 1952. He received the M.Sc. degree in theoretical physics from Utrecht University, Utrecht, The Netherlands, in 1976, and the Ph.D. degree (*cum laude*) from the Delft University of Technology, Delft, The Netherlands, in 1987.

From 1976 to 1986 and 1986 to 1993, he was an Assistant and Associate Professor with the Laboratory of Electromagnetic Research, Faculty of Electrical Engineering, Delft University of Technology. In 1993, he became a Full Professor of electromagnetics with the Faculty of Electrical Engineering, Eindhoven University of Technology, Eindhoven, The Netherlands. He has been a Visiting Scientist with the University of Colorado at Boulder, the University of Granada, Granada, Spain, the University of Tel Aviv, Tel Aviv, Israel, and with McDonnell Douglas Research Laboratories, St. Louis, MO. Since 1996, he has been a Consultant with TNO Defence, Security, and Safety, The Hague, The Netherlands. His research interests are the analytical, numerical, and physical aspects of the theory of electromagnetic waves. In particular, he is involved with efficient techniques for the computational modeling of electromagnetic fields and their application to detection and synthesis problems from several areas of electrical engineering.